

From Functional Phospholide Ions to Bifunctional 1,1'-Diphosphaferrocenes

Aholibama Escobar, Bruno Donnadiou, and François Mathey*

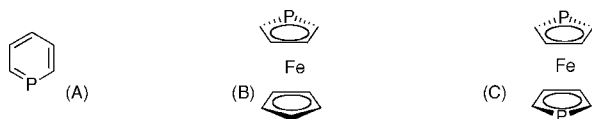
UCR-CNRS Joint Research Chemistry Laboratory, Department of Chemistry, University of California Riverside, Riverside, California 92521-0403

Received December 13, 2007

Both the 2-ethoxycarbonyl and the 2-benzoyl phospholides (**1** and **2**) react with FeCl₂ in the presence of ZnCl₂ to give the corresponding 2,2'-difunctional 1,1'-diphosphaferrocenes as mixtures of *meso* and *rac* diastereomers. Stable rotamers are also detected by ¹H and ¹³C NMR spectroscopy. Under the same conditions, the 2,5-bis(ethoxycarbonyl)phospholide (**3**) gives the tetrafunctional 1,1'-biphospholyl (**6**). The diphosphaferrocenes and the 1,1'-biphospholyl are probably formed from a common type of intermediates with a bis(η¹-phospholyl)iron structure. DFT computations indicate that this kind of intermediate is pyramidal at P and only weakly aromatic.

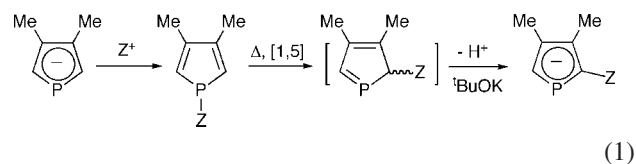
Introduction

Together with phosphinines (A), phosphoferrocenes (B) and 1,1'-diphosphaferrocenes (C) are certainly the most accessible and representative species incorporating a sp²-phosphorus center into an aromatic system. In all of these cases, the parent species are isolable^{1,2} because the aromatic stabilization energy eliminates the need for kinetic stabilization by bulky substituents, as is the case for phosphalkenes. This situation is exceptionally favorable since it has been demonstrated that bulky substituents significantly alter the chemistry of low-coordinate phosphorus centers.³



Phosphoferrocenes have already found interesting applications as ligands for transition metals in homogeneous catalysis.⁴ A logical further development of their chemistry would be to incorporate them into macrocyclic structures. The phosphinine ring has indeed been incorporated into macrocyclic structures,⁵ and the resulting macrocycles have shown an exceptional ability to stabilize low oxidation state metallic centers.⁶ A prerequisite for the synthesis of phosphoferrocene-based macrocycles is an

easy access to difunctional phosphoferrocenes. Aside from silyl-substituted derivatives,⁷ the only described difunctional derivative is a 2,2'-diacetyl-1,1'-diphosphaferrocene obtained by Friedel–Crafts acetylation of a nonfunctional diphosphaferrocene.² Some time ago, we devised a synthesis of functional phospholide ions based on the [1,5] shift of the functional group from P to C_α (eq 1).⁸



The simplicity of this one-pot synthesis of functional phospholides is quite attractive, and it was tempting to investigate their reaction with iron(II) derivatives in order to get bifunctional phosphoferrocenes. In this context, we were intrigued by a report of Ganter et al.⁷ stating that they had been unable to convert 2,5-difunctional phospholide ions into the corresponding Fe or Ru sandwich complexes. We thus decided to investigate this reaction more closely.

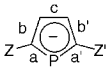
Results and Discussion

This work being focused on carbonyl functionalities, we first decided to investigate the influence of a carbonyl substituent on the electronic structure of a phospholide ion. A comparative theoretical study was carried out on the parent phospholide (D), the 2-formylphospholide (E), and the 2,5-diformylphospholide (F) by DFT at the B3LYP/6-311G++(3df,2p) level.⁹ The counterion was not included since it has been shown previously that it has only a limited influence on the structure of the anion.¹⁰ The results are collected in Table 1. Grafting one or two carbonyls on the ring significantly alters its structure. Anions

(1) Ashe, A. J., III *J. Am. Chem. Soc.* **1971**, *93*, 3293.
 (2) De Lauzon, G.; Deschamps, B.; Fischer, J.; Mathey, F.; Mitschler, A. *J. Am. Chem. Soc.* **1980**, *102*, 994.
 (3) Nyulaszi, L. *J. Organomet. Chem.* **2005**, *690*, 2597.
 (4) (a) Qiao, S.; Fu, G. C. *J. Org. Chem.* **1998**, *63*, 4168. (b) Tanaka, K.; Qiao, S.; Tobisu, M.; Lo, M. M.-C.; Fu, G. C. *J. Am. Chem. Soc.* **2000**, *122*, 9870. (c) Shintani, R.; Fu, G. C. *J. Am. Chem. Soc.* **2003**, *125*, 10778. (d) Ogasawara, M.; Yoshida, K.; Hayashi, T. *Organometallics* **2001**, *20*, 3913. (e) Suarez, A.; Downey, C. W.; Fu, G. C. *J. Am. Chem. Soc.* **2005**, *127*, 11244. (f) Ogasawara, M.; Ito, A.; Yoshida, K.; Hayashi, T. *Organometallics* **2006**, *25*, 2715.
 (5) (a) Avarvari, N.; Mézailles, N.; Ricard, L.; Le Floch, P.; Mathey, F. *Science* **1998**, *280*, 1587. (b) Avarvari, N.; Maigrot, N.; Ricard, L.; Mathey, F.; Le Floch, P. *Chem.-Eur. J.* **1999**, *5*, 2109.
 (6) Mézailles, N.; Avarvari, N.; Maigrot, N.; Ricard, L.; Mathey, F.; Le Floch, P.; Cataldo, L.; Berclaz, T.; Geoffroy, M. *Angew. Chem., Int. Ed.* **1999**, *38*, 3194.

(7) (a) Sava, X.; Mézailles, N.; Maigrot, N.; Nief, F.; Ricard, L.; Mathey, F.; Le Floch, P. *Organometallics* **1999**, *18*, 4205. (b) Loschen, R.; Loschen, C.; Frank, W.; Ganter, C. *Eur. J. Inorg. Chem.* **2007**, 553.
 (8) (a) Holand, S.; Jeanjean, M.; Mathey, F. *Angew. Chem., Int. Ed. Engl.* **1997**, *36*, 98. (b) Review: Mathey, F. *Acc. Chem. Res.* **2004**, *37*, 954.

Table 1. Computed Data on Phospholides

	a(a')	b(b')	c	NICS(1) ^a	Charge at P ^b	Charge at O ^b	π sym (eV)	π asym (eV)	I.p. (eV)
Z,Z'=H (D)	1.764	1.393	1.413	-10.86	-0.43	-	-0.24	-0.84	-2.04
Z=CHO, Z'=H (E)	1.786 (1.743)	1.414 (1.408)	1.391	-10.18	-0.24	-0.69	-1.09	-1.74	-2.37
Z,Z'=CHO (F)	1.766	1.421	1.378	-10.09	-0.09	-0.67	-1.77	-2.48	-2.99

^aRHF/6-311+G**; see ref 11. ^bMulliken.

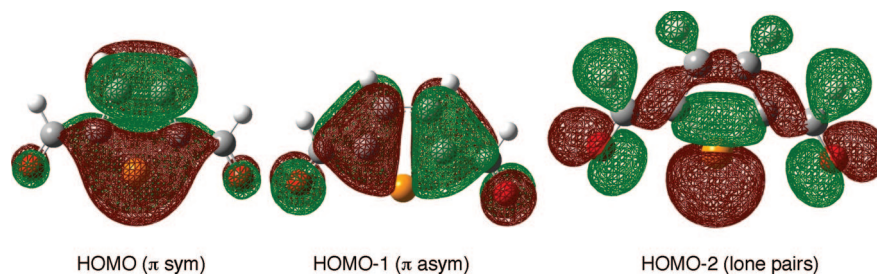
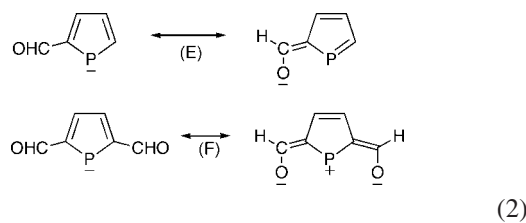


Figure 1. Highest occupied orbitals of anion F.

E and F are better represented by the mesomeric formulations shown in eq (2).



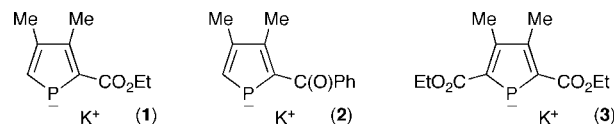
The negative charge at P sharply decreases from D to E and F, but the aromaticity does not according to the NICS(1) index. The highest occupied orbitals are shown in Figure 1 for F. The HOMO and HOMO-1 that are involved in the π -bonding with Fe(II) are shifted to lower energies to such an extent that π_{asym} is lower for F than the lone pair orbital for D. This casts some doubt on the ability of F to give a stable π -complex with iron. Indeed, the energetic gap between these orbitals and the d_{xz} and d_{yz} orbitals of iron might become too large to allow the formation of a stable η^5 -structure.

(9) Frisch, M. J.; Trucks, G. W.; Schlegel, H. B.; Scuseria, G. E.; Robb, M. A.; Cheeseman, J. R.; Montgomery, J. A., Jr.; Vreven, T.; Kudin, K. N.; Burant, J. C.; Millam, J. M.; Iyengar, S. S.; Tomasi, J.; Barone, V.; Mennucci, B.; Cossi, M.; Scalmani, G.; Rega, N.; Petersson, G. A.; Nakatsuji, H.; Hada, M.; Ehara, M.; Toyota, K.; Fukuda, R.; Hasegawa, J.; Ishida, M.; Nakajima, T.; Honda, Y.; Kitao, O.; Nakai, H.; Klene, M.; Li, X.; Knox, J. E.; Hratchian, H. P.; Cross, J. B.; Adamo, C.; Jaramillo, J.; Gomperts, R.; Stratmann, R. E.; Yazyev, O.; Austin, A. J.; Cammi, R.; Pomelli, C.; Ochterski, J. W.; Ayala, P. Y.; Morokuma, K.; Voth, G. A.; Salvador, P.; Dannenberg, J. J.; Zakrzewski, V. G.; Dapprich, S.; Daniels, A. D.; Strain, M. C.; Farkas, O.; Malick, D. K.; Rabuck, A. D.; Raghavachari, K.; Foresman, J. B.; Ortiz, J. V.; Cui, Q.; Baboul, A. G.; Clifford, S.; Cioslowski, J.; Stefanov, B. B.; Liu, G.; Liashenko, A.; Piskorz, P.; Komaromi, I.; Martin, R. L.; Fox, D. J.; Keith, T.; Al-Laham, M. A.; Peng, C. Y.; Nanayakkara, A.; Challacombe, M.; Gill, P. M. W.; Johnson, B.; Chen, W.; Wong, M. W.; Gonzalez, C.; Pople, J. A. *Gaussian 03*, Revision B.05; Gaussian, Inc., Pittsburgh, PA, 2003.

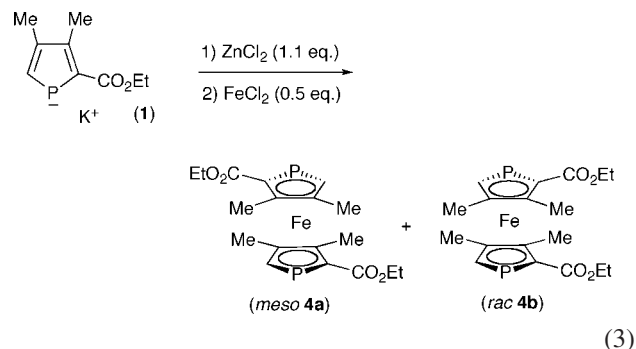
(10) Grundy, J.; Donnadiu, B.; Mathey, F. *J. Am. Chem. Soc.* **2006**, *128*, 7716.

(11) Chen, Z.; Wannere, C. S.; Corminboeuf, C.; Puchta, R.; Schleyer, P. v. R. *Chem. Rev.* **2005**, *105*, 3842.

For our experimental work, we chose to investigate the reaction of the three easily accessible functional phospholides **1–3**^{8,12} with FeCl₂. Our initial experiments were carried out with **1**.



The reaction of **1** with FeCl₂ in THF at RT afforded only a complex mixture of decomposition products. We suspected that Fe(II) was partly reduced by the anion, and we chose to reduce the ionicity of the potassium phospholide by metathesis with ZnCl₂. The zinc phospholide cleanly reacted with FeCl₂ to give a 70:30 mixture of the expected *meso* (**4a**) ($\delta^{31}\text{P}$ -45.9 ppm) and *rac* (**4b**) ($\delta^{31}\text{P}$ -50.5 ppm) difunctional 1,1'-diphosphaferecenes (eq 3).



After a preliminary purification by chromatography, the pure *meso* diastereomer was obtained in the pure state by extraction with pentane. The X-ray crystal structure of **4a** is shown in Figure 2. The two phospholyl rings are in a head-to-tail disposition. The carbonyls are lying in the planes of the rings and are directed toward the methyl substituents. The ¹H NMR

(12) Toullec, P.; Mathey, F. *Synlett* **2001**, 1977.

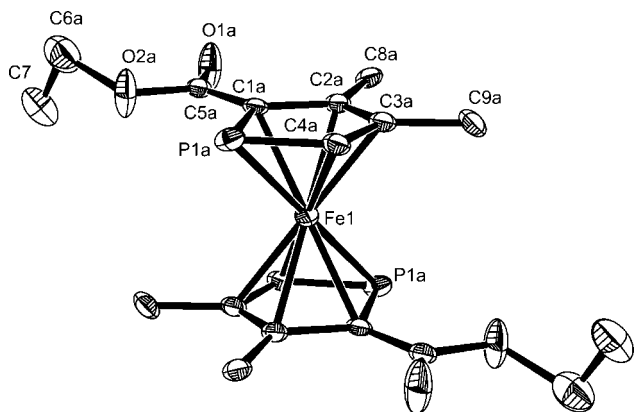
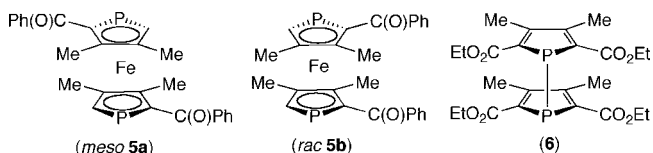


Figure 2. X-ray crystal structure of *meso*-2,2'-bis(ethoxycarbonyl)-1,1'-diphosphaferrocene (**4a**). Ellipsoids are scaled to enclose 50% of the electronic density. Main bond lengths (Å) and angles (deg): P1–C1 1.87(5), P1–C4 1.76(5), C1–C2 1.451(16), C2–C3 1.407(18), C3–C4 1.374(18), Fe1–C1 2.11(5), Fe1–C4 2.04(3), Fe1–P1 2.221(38); C1–P1–C4 86(2).

spectrum shows two types of ethyl groups whose methyl resonances appear at 0.88 (37%) and 1.05 ppm (63%). These methyl resonances are correlated with two closely spaced ^{13}C resonances at 14.31 (minor) and 14.41 ppm (major). Two sets of OCH_2 resonances also appear on the ^1H spectrum, but they are very close. We interpret this phenomenon as resulting from the presence of two stable rotamers. In the minor one, the carbonyls would lie opposite of the methyl substituents. Upon heating at 60–70 °C, the minor rotamer is slowly and irreversibly transformed into the major one. We prefer this explanation rather than the other possibility involving a blocked rotation around the Fe axis because only the ethyl resonances are different in the two rotamers.

Using the same experimental protocol, we were able to prepare the 2,2'-dibenzoyl-1,1'-diphosphaferrocene (**5**) from the functional phospholide **2**. Like **4**, **5** is obtained as a mixture of *meso* (**5a**) and *rac* (**5b**) diastereomers.



The ^1H and ^{13}C NMR spectra show that **5b** is a mixture of two rotamers.

Always using the same protocol, the reaction of the difunctional phospholide **3** with FeCl_2 yielded the tetrafunctional biphospholyl **6** in 20% overall yield. Due to the paramagnetism of the solution, it proved impossible to monitor the reaction by ^{31}P NMR. However, after filtration on silica gel, we checked that **6** was the sole important product and that no diphosphaferrocene was formed. Obviously, the modest overall yield partly reflects the moderate yield of the functionalization step. The X-ray crystal structure of **6** is shown in Figure 3. The P–P distance is normal at 2.2289(14) Å. The two rings are in a staggered conformation. The phosphorus atoms are highly pyramidal; Σ angles at P = 290.9°. The strong alternation between the C–C single and the C=C double bonds of the rings confirms the absence of electronic delocalization. The carbonyls are directed toward the methyl substituents but are not coplanar with the rings.

These results suggest that the reaction of phospholides with FeCl_2 proceeds via a σ P–Fe complex such as **7** (eq 4). A η^1

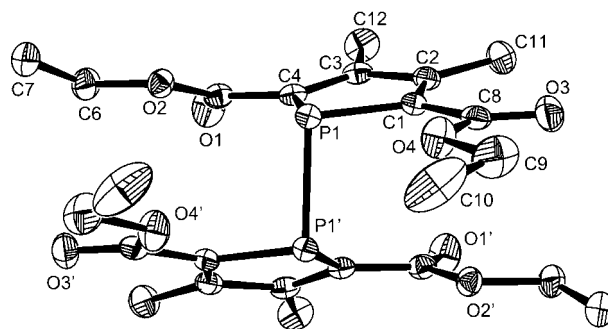
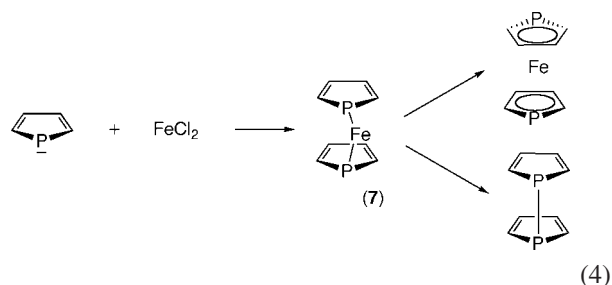


Figure 3. X-ray crystal structure of 3,3',4,4'-tetramethyl-2,2',5,5'-tetrakis(ethoxycarbonyl)-1,1'-biphospholyl (**6**). Ellipsoids are scaled to enclose 50% of the electronic density. Main bond lengths (Å) and angles (deg): P1–P1' 2.2289(14), P1–C1 1.809(2), P1–C4 1.805(4), C1–C2 1.358(4), C2–C3 1.466(4), C3–C4 1.362(3); C1–P1–C4 89.66(11), C1–P1–P1' 98.29(9), C4–P1–P1' 102.95(8).

$\rightarrow \eta^5$ fluctuation would yield the diphosphaferrocene, whereas a reductive elimination would yield the 1,1'-biphospholyl.



In order to give some support to this proposition, we decided to compute the structure of **7** with two molecules of THF as additional ligands. The computation was carried out by DFT at the B3LYP/6-31G(d) (C, H, O, P) and lan2dz (Fe) level. The computed structure is shown in Figure 4. It corresponds to a genuine minimum (no negative frequency). The most interesting feature is that the phosphorus atoms are pyramidal (Σ angles at P = 336.9°), although less than in a normal phosphole. As a result, the phosphole ring is poorly delocalized and a strong alternation between the single and the double bonds is still present (1.443 vs 1.370 Å). We note a good agreement with the X-ray crystal structure analysis of a η^1 -phospholyltungsten complex.¹³ One of the driving forces for the formation of the diphosphaferrocene is thus the aromatization of the rings during the $\eta^1 \rightarrow \eta^5$ fluctuation. Such a driving force does not exist in the case of pyrrolyl complexes (both η^1 - and η^5 -pyrrolyl complexes are aromatic), and this might explain why diazaferrocenes are more difficult to prepare than diphosphaferrocenes.¹⁴

Experimental Section

Nuclear magnetic resonance spectra were obtained on Bruker Avance 300 and Varian Inova spectrometers operating at 300.13 MHz for ^1H , 75.45 MHz for ^{13}C , and 121.496 MHz for ^{31}P . A Bruker Avance 600 instrument was also used for ^1H and ^{13}C (150.925 MHz) spectra. Chemical shifts are expressed in parts per

(13) Mercier, F.; Ricard, L.; Mathey, F. *Organometallics* **1993**, *12*, 98.

(14) Kuhn, N.; Horn, E. M.; Boese, R.; Augart, N. *Angew. Chem., Int. Ed. Engl.* **1988**, *27*, 1368.

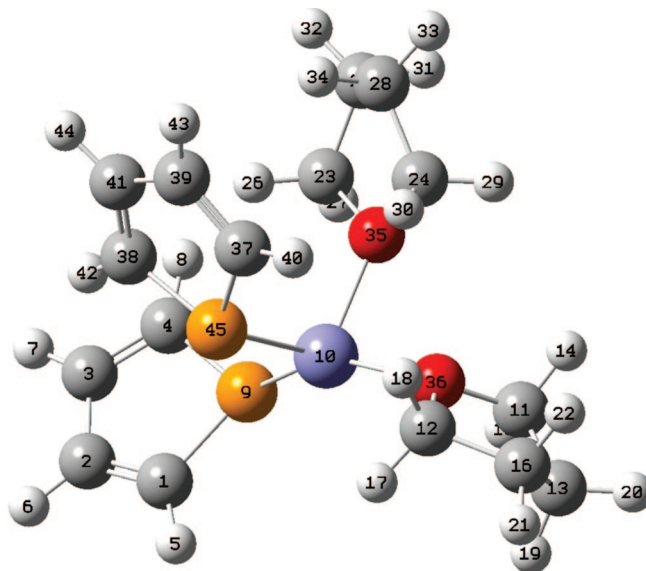


Figure 4. Computed structure of the σ -complex (7)(THF)₂. Main bond lengths (Å) and angles (deg): Fe–P9 2.278, P9–C1 1.791, P9–C4 1.792, C1–C2 1.369, C2–C3 1.443, C3–C4 1.370, Fe–P45 2.253; P9–Fe–P45 103.84, C1–P9–C4 91.08, C1–P9–Fe 115.35, C4–P9–Fe 130.44.

million downfield from external TMS (¹H and ¹³C) and external 85% H₃PO₄ (³¹P). Mass spectra were obtained on VG 7070 and Hewlett-Packard 5989A GC/MS spectrometers. Elemental analyses were performed by Desert Analytics Laboratory, Tucson, AZ.

3,3',4,4'-Tetramethyl-2,2'-bis(ethoxycarbonyl)-1,1'-diphosphaferrocene (4a,b). 1-Phenyl-3,4-dimethylphosphole (2 g, 10.63 mmol) in dry THF (25 mL) was allowed to react with an excess of lithium wire until the P–Ph bond cleavage was completed. After excess lithium was removed, the solution was treated with *tert*-butyl chloride (1.2 mL, 10.63 mmol) and heated to 60 °C for 1 h. Ethyl chloroformate (1.1 mL, 11.7 mmol) was added dropwise at –78 °C. The solution was heated at 65 °C for 2.5 h. *t*BuOK was added (1.3 g, 11.7 mmol) at 0 °C. The resulting mixture was heated at 60 °C for 2 h. ZnCl₂ (1.4 g, 10.63 mmol) was added at 0 °C and stirred at room temperature for 30 min. FeCl₂ (0.67 g, 5.3 mmol) was added at room temperature. The solution was stirred for 18 h at RT. The crude solution mixture was filtered through silica and concentrated. Purification was performed via column chromatography on silica using 3:2 dichloromethane/petroleum ether. A red band was collected and, once concentrated, 683 mg of a red solid was obtained (30% yield). The *meso* diastereomer was extracted from the solid with pentane and crystallized from the pentane solution. We were unable to get the *rac* diastereomer in the pure form.

meso Diastereomer (4a). ³¹P NMR (C₆D₆): δ –45.3. ¹H NMR (C₆D₆): δ 0.88 (t, Me(Et) minor), 1.05 (t, Me(Et) major), 1.78 (s, Me), 2.40 (s, Me), 3.72 (d, ²J_{HP} = 36.4 Hz, CH–P), 4.04 (2q, OCH₂). ¹³C NMR (C₆D₆): δ 13.54 (s, Me), 14.41 (s, Me(Et)), 15.17 (s, Me), 60.30 (s, OCH₂), 84.40 (d, ¹J_{C–P} = 62.3 Hz, =C–P), 86.45 (d, ¹J_{C–P} = 58.7 Hz, =CH–P), 98.74 (d, ²J_{CP} = 5.2 Hz, =C(Me)), 102.64 (d, ²J_{CP} = 9.0 Hz, =C(Me)), 171.32 (d, ²J_{CP} = 19.8 Hz, CO). MS (EI): *m/z* 422 (M⁺, 100%). Anal. Calcd for C₁₈H₂₄FeO₄P₂: C, 51.21; H, 5.73. Found: C, 50.79; H, 5.79.

3,3',4,4'-Tetramethyl-2,2'-dibenzoyl-1,1'-diphosphaferrocene (5a,b). 1-Phenyl-3,4-dimethylphosphole (2 g, 10.63 mmol) in dry THF (25 mL) was allowed to react with an excess of lithium wire until the P–Ph bond cleavage was completed. After excess lithium was removed, the solution was treated with *tert*-butyl chloride (1.2 mL, 10.63 mmol) and heated at 60 °C for 1 h. Benzoyl chloride (1.4 mL, 11.7 mmol) was added dropwise at –78 °C. The mixture was warmed to room temperature and stirred for 20 min.

*t*BuOK (1.3 g, 11.7 mmol) was added at 0 °C, and the solution was stirred at 60 °C for 2 h. The solution was cooled to 0 °C, ZnCl₂ (1.4 g, 10.63 mmol) was added, and the mixture was stirred at room temperature for 30 min. FeCl₂ (0.67 g, 5.3 mmol) was added, and the solution was stirred for 18 h. The crude reaction mixture was filtered through silica and concentrated. Purification was performed via column chromatography on silica using 3:2 petroleum ether/dichloromethane solution. A red band was collected and, once concentrated, 863 mg of a red oil was obtained (33% yield). The two diastereomers were separated by a second chromatography with methylene chloride as the eluent and crystallized upon slow evaporation of the solvent.

meso Diastereomer (5a). ³¹P NMR (C₆D₆): δ –53.1. ¹H NMR (C₆D₆): δ 1.88 (s, Me), 2.10 (s, Me), 3.93 (m, CH–P), 6.98–7.16 (m, Ph), 7.86 (m, Ph *ortho*). ¹³C NMR (C₆D₆): δ 11.40 (s, Me), 12.60 (s, Me), 83.68 (m, =CH–P), 91.34 (m, =C–P), 98.93 (d, =C(Me)), 101.70 (d, =C(Me)), 139.26 (s, Ph *ipso*C), 197.68 (pseudo t, CO).

rac Diastereomers (5b1 and 5b2): 5b1 (major). ³¹P NMR (C₆D₆): δ –43.7. ¹H NMR (C₆D₆): δ 1.87 (s, Me), 2.09 (s, Me), 4.09 (d, ²J_{HP} = 45 Hz, CH–P), 7.84 (m, Ph *ortho*). ¹³C NMR (C₆D₆): δ 13.14 (s, Me), 14.37 (s, Me), 87.69 (d, ¹J_{CP} = 74.7 Hz, =CH–P), 96.68 (d, ¹J_{CP} = 79.7 Hz, =C–P), 100.66 (s, =C(Me)), 103.45 (d, ²J_{CP} = 5.0 Hz, =C(Me)), 141.14 (s, Ph *ipso*C), 199.04 (d, ²J_{CP} = 22.3 Hz, CO).

5b2 (minor). ³¹P NMR (C₆D₆): δ –43.4. ¹H NMR (C₆D₆): δ 2.07 (s, Me), 2.26 (s, Me), 3.92 (m, CH–P), 7.80 (m, Ph *ortho*). ¹³C NMR (C₆D₆): δ 15.39 (s, Me), 16.49 (s, Me), 85.31 (m, =CH–P), 93.09 (m, =C–P), 99.90 (d, ²J_{CP} = 5.0 Hz, =C(Me)), 102.57 (d, ²J_{CP} = 10.0 Hz, =C(Me)), 141.01 (s, Ph *ipso*C), 199.44 (pseudo t, CO). Anal. Calcd for C₂₆H₂₄FeO₂P₂: C, 64.22; H, 4.97. Found: C, 64.39; H, 4.94.

3,3',4,4'-Tetramethyl-2,2',5,5'-tetrakis(ethoxycarbonyl)-1,1'-biphospholyl (6). 1-Phenyl-3,4-dimethylphosphole (2 g, 10.63 mmol) in dry THF (25 mL) was allowed to react with an excess of lithium wire until the P–Ph bond cleavage was complete. After excess lithium was removed, the solution was treated with *tert*-butyl chloride (1.2 mL, 10.63 mmol) and heated to 60 °C for 1 h. Ethyl chloroformate (1.1 mL, 11.7 mmol) was added dropwise at –78 °C. The solution was heated at 65 °C for 2.5 h. *t*BuOK was added (1.4 g, 12.8 mmol) at 0 °C, followed by heating at 60 °C for 2 h. A second equivalent of ethyl chloroformate (1.2 mL, 12.8 mmol) was added at –78 °C, immediately followed by addition of a second equivalent of *t*BuOK (1.4 g, 12.8 mmol) at 0 °C. The resulting mixture was stirred at 40 °C for 18 h. The solution was cooled to 0 °C, ZnCl₂ (1.4 g, 10.63 mmol) was added, and the mixture was stirred at room temperature for 30 min. FeCl₂ (0.67 g, 5.3 mmol) was added, and the mixture was stirred for 18 h. The crude reaction mixture was filtered through silica and concentrated. Purification was performed via column chromatography on silica using 100:1 dichloromethane/ethyl acetate solution. A yellow band was collected and, once concentrated, 542 mg of a yellow solid was obtained (20% yield). The yellow solid was recrystallized from dichloromethane.

³¹P NMR (CD₂Cl₂): δ –6.5. ¹H NMR (CD₂Cl₂): δ 1.29 (t, Me(Et)), 2.34 (m, Me–C=), 4.07 (m, OCH₂), 4.20 (m, OCH₂). ¹³C NMR (CD₂Cl₂): δ 14.57 (s, Me(Et)), 15.82 (s, Me–C=), 61.18 (s, OCH₂), 136.32 (pseudo t, C α), 158.12 (pseudo t, C β), 165.00 (pseudo t, CO). MS (EI): *m/z* 510 (M, 80%), 254 (M/2, 100%). The compound is sensitive to oxidation. Anal. Calcd for C₂₄H₃₂O₈P₂: C, 56.47; H, 6.32. Found: C, 56.2; H, 6.3.

X-Ray Structure Determination of 4a and 6. Compounds were measured at low temperature, *T* = 100(2) K, on a X8-APEX Bruker Kappa four-circle X-ray diffractometer system (Mo radiation, λ = 0.71073 Å). An optimized data collection strategy was defined using

Cosmo.¹⁵ Frames were integrated with the aid of Bruker Saint software¹⁶ included in the Bruker APEX2 package¹⁷ and using a narrow-frame integration algorithm.

4a: The integrated frames yielded a total of 3925 reflections at a maximum 2θ angle of 43.94° , of which 1127 were independent reflections ($R_{\text{int}} = 0.0814$, $R_{\text{sig}} = 0.0895$, completeness = 98.5%) and 871 (77.28%) reflections were greater than $2\sigma(I)$. A triclinic cell space group $P2(1)/n$ was found; the unit cell parameters were $a = 6.796(5)$ Å, $b = 8.163(6)$ Å, $c = 16.939(13)$ Å, $\alpha = 90.0^\circ$, $\beta = 96.360(9)^\circ$, $\gamma = 90.0^\circ$, $V = 933.9(12)$ Å³, $Z = 4$, calculated density $D_c = 1.473$ Mg/m³. The molecule is statistically disordered on two positions.

6: The integrated frames yielded a total of 6858 reflections at a maximum 2θ angle of 46.50° , of which 1835 were independent reflections ($R_{\text{int}} = 0.0307$, $R_{\text{sig}} = 0.0294$, completeness = 99.4%) and 1617 (88.12%) reflections were greater than $2\sigma(I)$. A monoclinic cell space group $C2/c$ was found; the unit cell parameters were $a = 20.816(5)$ Å, $b = 10.489(2)$ Å, $c = 12.513(3)$ Å, $\beta = 109.335(3)^\circ$, $V = 2578.2(10)$ Å³, $Z = 8$, calculated density $D_c = 1.315$ Mg/m³.

6 is organized around a $C2$ axis with the following symmetry transformations used to generate equivalent atoms: #1 $-x, y, -z+3/2$.

Absorption corrections were applied for data using the SADABS¹⁸ program. The program SIR92¹⁹ was used for phase

determination and structure solution, followed by some subsequent differences Fourier maps. From the primary electron density map most of the non-hydrogen atoms were located, and with the aid of subsequent isotropic refinement all of the non-hydrogen atoms were identified. Atomic coordinates and isotropic and anisotropic displacement parameters of all the non-hydrogen atoms were refined by means of a full matrix least-squares procedure on F^2 . The H atoms were included in the refinement in calculated positions riding on the C atoms to which they were attached. The refinement converged for **4a** at $R1 = 0.0751$, $wR2 = 0.1862$, with intensity $I > 2\sigma(I)$, and for **6** at $R1 = 0.0406$, $wR2 = 0.1057$ with intensity $I > 2\sigma(I)$.

Drawings of molecules were performed using ORTEP32.²⁰ (Further details on the Crystal Structure Investigation are available on request from the Director of the Cambridge Crystallographic Data Centre, 12 Union Road, GB-Cambridge CB21EZ UK, on quoting the full journal citation.)

Acknowledgment. The authors thank the University of California Riverside and the CNRS (Paris) for financial support.

Supporting Information Available: X-ray crystal structure analyses of compounds **4a** and **6**. This material is available free of charge via the Internet at <http://pubs.acs.org>.

OM7012474

(15) COSMO version 1.53; Bruker AXS Inc.: Madison, WI, 2004.
(16) SAINT version V7.06A; Bruker AXS Inc.: Madison, WI, 2003.
(17) APEX 2 version 2.0-2; Bruker AXS Inc.: Madison, WI, 2004.
(18) SADABS version 2004/1; Bruker AXS Inc.: Madison, WI, 2004.
(19) SIR92-A program for crystal structure solution. Altomare, A.; Cascarano, G.; Giacovazzo, C.; Guagliardi, A. *J. Appl. Crystallogr.* **1993**, *26*, 343-350.

(20) ORTEP3 for Windows. Farrugia, L. J. *J. Appl. Crystallogr.* **1997**, *30*, 565.